Cell Stem Cell
Short Article

Spindle Orientation Bias in Gut Epithelial Stem Cell Compartments Is Lost in Precancerous Tissue

Aaron J. Quyn,[1,2] Paul L. Appleton,[1] Francis A. Carey,[3] Robert J.C. Steele,[2] Nick Barker,[4] Hans Clevers,[4] Rachel A. Ridgway,[5] Owen J. Sansom,[5] and Inke S. Näthke[1,*]
[1]Cell and Developmental Biology, University of Dundee, Dundee, DD1 5EH, UK
[2]Surgery and Molecular Oncology
[3]Pathology and Neuroscience
Ninewells Hospital and Medical School, University of Dundee, Dundee, DD1 9SY, UK
[4]Hubrecht Laboratory, KNAW Postbus 85164, Utrecht AD 3508, Netherlands
[5]Beatson Institute for Cancer Research, Glasgow, G611BD, UK
*Correspondence: i.s.nathke@dundee.ac.uk
DOI 10.1016/j.stem.2009.12.007

SUMMARY

The importance of asymmetric divisions for stem cell function and maintenance is well established in the developing nervous system and the skin; however, its role in gut epithelium and its importance for tumorigenesis is still debated. We demonstrate alignment of mitotic spindles perpendicular to the apical surface specifically in the stem cell compartments of mouse and human intestine and colon. This orientation correlates with the asymmetric retention of label-retaining DNA. Both the preference for perpendicular spindle alignment and asymmetric label retention are lost in precancerous tissue heterozygous for the adenomatous polyposis coli tumor suppressor (*Apc*). This loss correlates with cell shape changes specifically in the stem cell compartment. Our data suggest that loss of asymmetric division in stem cells might contribute to the oncogenic effect of *Apc* mutations in gut epithelium.

INTRODUCTION

Cells in the gut are continually exposed to damage-inducing factors. This imposes the need for mechanisms to protect long-lived stem cells. The large number of progeny these cells produce makes it imperative to maintain their genetic stability and prevent DNA damage. A recent report showing that mutations in the adenomatous polyposis coli gene (*Apc*) produce tumors much more efficiently when initiated in the stem cell compartment in the intestine than in the transit-amplifying compartment suggests strongly that Apc is crucial for normal maintenance of stem cell populations (Barker et al., 2009). One mechanism to minimize DNA damage in stem cells is described by Cairns' Hypothesis, which proposes that stem cells retain unreplicated DNA strands to minimize mutations introduced by replication errors (Cairns, 1975). Asymmetric cell division and a corresponding alignment of mitotic spindles is key to any mechanism that achieves this retention and abolishing such protection may be an important contributing factor in the development of cancer.

The specific environment experienced by stem cells provides critical spatial and biochemical information for their behavior. This makes it imperative to examine stem cells in their usual physiological context. The inherent difficulty in imaging opaque biological tissue has made any in vivo analysis of stem cells in adult tissue technically challenging. Furthermore, the three-dimensional organization of intestinal crypts makes them particularly inaccessible: they can be up to 200 μm deep in mouse (even longer in human), 40–60 μm in diameter, and are tightly packed into regular arrays. Thus gaining detailed insights into three-dimensional cellular architecture from two-dimensional histological sections is difficult. We measured spindle orientation in three dimensions in whole-mount samples of gut epithelium from wild-type and *Apc* heterozygous ($Apc^{Min/+}$) mice. Previous reports of spindle orientation in wild-type and $Apc^{Min/+}$ mouse intestinal epithelium were based on 8–10 μm sections and describe only transit-amplifying cells (Bjerknes and Cheng, 1989; Caldwell et al., 2007; Fleming et al., 2007). However, to determine spindle orientation in relation to crypt architecture and to validate and integrate cell biological and visual data, it is necessary to image such samples in toto (Bjerknes and Cheng, 1989). In addition, examining 8 μm sections limits the mitotic spindles that can be scored to spindle for which both poles are visible in the section. Thus, previous approaches could provide only a limited representation.

We used high-resolution multiphoton microscopy to determine spindle orientation of dividing cells in small intestine and colon in three dimensions and compared divisions in the stem cell and transit-amplifying compartments of wild-type and *Apc* heterozygous and homozygous mutant human and mouse tissue (Appleton et al., 2009).

RESULTS

Definition of Stem Cell Compartment

To define stem cell and transit-amplifying compartments in the gut for our analysis, and to differentiate stem from other cells

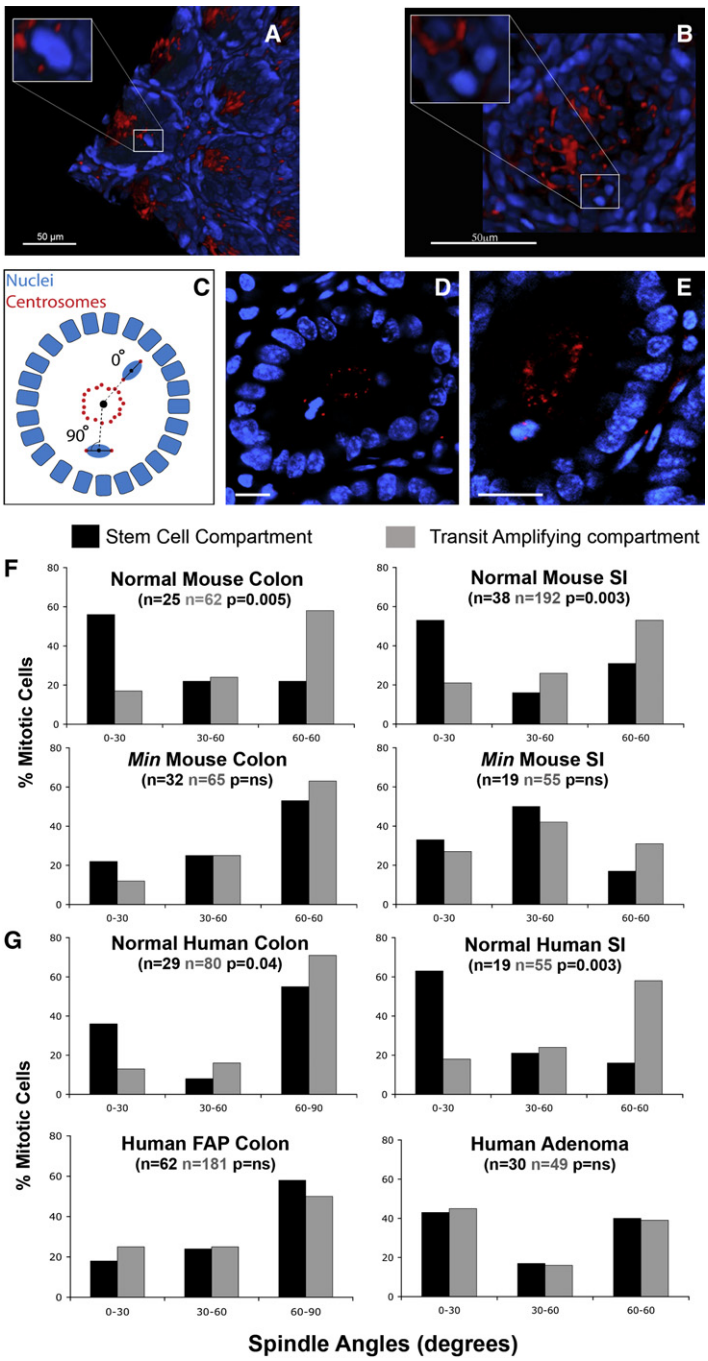

Figure 1. Mitotic Spindles Orient Preferentially Perpendicular to the Apical Surface in the Stem Cell Compartment of Normal but Not *Apc* Heterozygous Human and Mouse Intestine

(A, D, E) Immunoflourescent multiphoton microscopy was used to visualize centrosomes labeled with pericentrin antibodies (red), which marks spindle poles, and DNA (DAPI) (blue).

(B) PAR-3 (red) localizes to the apical border of crypt cells and maintains this position during mitosis, independently of mitotic plane in wild-type (shown here) and $Apc^{Min/+}$ mouse intestine.

Scale bars represent 50 μm.

(C) Schematic to illustrate how angles were defined.

(F and G) Cells in the stem cell compartment (black bars) of mouse (F) and human (G) colon and small intestine preferentially align their mitotic spindles perpendicular to the apical surface unlike cells in the transit-amplifying compartment (gray bars). The graph represents the cumulative results from four wild-type mice, four $Apc^{Min/+}$ littermates, and four human patients, two FAP patients with mutations that led to truncations after nucleotide 5979 and 5772, and in three human adenomas from separate patients. Previous studies showed that adenomas invariably show loss of *Apc* either by allelic loss, mutation, or epigenetic silencing (Judson et al., 2006). Thus, all of the tumors analyzed were assumed to express only truncated *Apc*. p values for the significance of the difference between SCC and TAC are shown in each panel. SI, small intestine.

See also Figures S1 and S2.

in the crypt, stem cells were visualized with LGR5-GFP (Barker et al., 2007). In the small intestine, cells expressing LGR5 reside between fully differentiated Paneth cells and also populate positions 1 to 4 or 7 in many cases (Figure S1A available online). In the colon, where there are no Paneth cells, LGR5 was present in most cells between position 1 and 4 and in many cases up to position 7 (Figure S1B). Based on these observations, we defined the bottom of crypts up to position 7 as the stem cell compartment (SCC) and the region above this as the transit-amplifying compartment (TAC). With this definition, each mitotic cell along the crypt was scored by examination of three-dimensional stacks (Figures S1C and S1D).

This classification ensured inclusion of all cells that have been identified as potential stem cells based on different stem cell markers (Potten et al., 2009). This may have introduced some bias, because it is likely that the stem cell compartment as defined for this study was "diluted" with some transit-amplifying or intermediate progenitor cells. Nonetheless, this definition distinguishes between compartments that do or do not contain all stem cells.

Mitotic Spindles Orient Perpendicular to the Apical Surface Specifically in the Stem Cell Compartment of Gut Epithelium

Mitotic spindles were visualized in three dimensions in intestinal and colonic whole-mount tissue stained with DNA dyes and antibodies that mark centrosomes (Figures 1A and 1B; Figures S1C–S1H). Mitotic cells were identified based on a number of criteria: the displacement of a mitotic nucleus toward the apical surface, its appearance as condensed (both are different in apoptotic cells), and the presence of two pericentrin-positive spots, which tend to be brighter in mitosis and in different positions than in nonmitotic cells (Figures 1A and 1B; Figures S1E–S1H). Only cells for which these criteria were met were used. Marking mitotic cells with anti-phospho-Histone 3 antibodies would have missed cells in later stages of mitosis because dephosphorylation of Histone 3 in early anaphase precludes its reliable detection at later stages of mitosis and ~50% of all mitoses we scored were in ana- or telophase (data not shown) (Hans and Dimitrov, 2001).

The position of each mitotic cell along the crypt axis was recorded as a function of position from the bottom of the crypt (Figures S1C and S1D). With three-dimensional images, mitotic

orientation was scored visually or calculated by a mathematical method that used the recorded spatial coordinates of spindle poles (marked by centrosomes; Figure 1A; Figures S1E–S1H) and the apical surface as reference point (as marked by PAR-3) (Figure 1B; Figure S2) to measure angles of spindle orientation. The axis that runs perpendicular to the apical surface of the epithelium within which the dividing cell lay was used as reference axis so that a mitotic spindle orientated toward the center of the crypt at an angle 0°–30° from this reference line was scored as perpendicular (Figure 1C).

The use of both the visual and mathematical methods to measure spindle orientation revealed differences between mitotic spindle orientation in the stem cell and the transit-amplifying compartment (Figure 1D). In wild-type mouse tissue, cells near the base of crypts tended to orient their spindles perpendicular to the apical surface of the epithelium (55%), whereas they oriented more parallel above position 7 (26% perpendicular). This was the case in small intestine and colonic crypts (Figure 1F). To determine whether cells maintained apical-basal polarity during mitosis and thus whether perpendicular orientation reflected an asymmetry in division, we examined the localization of PAR-3, an integral member of the PAR-aPKC complex (Ahringer, 2003). The localization of PAR-3 remained apical regardless of cell cycle stage or spindle orientation (Figure 1B; Figure S2).

To relate our results showing preferred perpendicular spindle alignment in intestinal stem cell compartments in mice to human tissue, we also measured spindle orientation and PAR-3 localization in normal human tissue samples. The relative difference between spindle orientation in stem cell and transit-amplifying compartments of human small intestine and colon was similar to that observed in mouse (small intestine, SCC 63% versus TAC 18%; colon, SCC 36% versus TAC 13%) (Figure 1G).

The Preferred Perpendicular Mitotic Alignment in the Stem Cell Compartment Is Lost in Precancerous and Cancerous Tissue

Mutations in the *Apc* tumor suppressor gene are the most prevalent initiating mutations in colorectal cancers and are also responsible for familial adenomatous polyposis (FAP). The Apc protein interacts with cytoskeletal proteins and these interactions may be altered even when *Apc* is heterozygous because interactions between N-terminal Apc fragments produced by mutated alleles may alter protein interactions of the remaining wild-type copy (Green et al., 2005; Li et al., 2008; Li and Näthke, 2005). Abnormalities in spindle orientation have indeed been described in the intestines of $Apc^{Min/+}$ mice; however, previous data examined only the transit-amplifying compartment (Caldwell et al., 2007; Fleming et al., 2007, 2009). Our high-resolution, three-dimensional analysis revealed no bias toward perpendicular spindle orientation in the stem cell compartment of $Apc^{Min/+}$ mouse intestine or FAP human intestine. Fewer cells in the stem cell compartment divided perpendicular to the apical surface in both $Apc^{Min/+}$ mouse and FAP tissue than in wild-type tissue (26% 0°–30° and 18% 0°–30°, respectively). The distribution of these angles is significantly different from those in the corresponding wild-type tissue ($p = 0.03$ for SCC in mouse small intestine, $p = 0.02$ for SCC in colon; p = not significant for all TAC comparisons) (Figure 1F). Importantly, the *Apc* truncation mutations in the FAP patients we used in our analysis lie beyond the 20 amino acid repeats and thus should not interfere with normal regulation of Wnt signaling. Polarity of dividing cells as marked by PAR-3 was the same in $Apc^{Min/+}$ tissue as in wild-type tissue (Figure 1; Figure S2).

We also measured spindle orientation in human adenomas. The pattern was similar to that observed in macroscopically normal human FAP tissue (Figure 1G). Despite the disordered architecture associated with adenomas, localization of PAR-3 to tight junctions indicated that cellular polarity was maintained (data not shown).

Perpendicularly Aligned Divisions Maintain Labeled DNA Strands Basally

To identify other markers of asymmetric cell division, we also examined the distribution of labeled DNA in dividing cells in the stem cell and transit-amplifying compartments. Mice were irradiated to eliminate stem cells in the gut, injected with EdU during the regeneration phase to label DNA, and then left to recover for 8 days. During this time, the label present in the majority of proliferating cells diluted to subthreshold levels, leaving EdU only in label-retaining cells (LRCs) in the base of the crypt. The elimination of stem cells and their subsequent recovery in response to this treatment was confirmed by (1) the disappearance of LGR5-GFP-positive cells after the irradiation and (2) the presence of EdU in non-Paneth cells at the base of crypts in cells at position 1–4 after the 8 day chase (Figure S4).

The distribution of LRCs along the crypt axis was similar to that in previously published reports that used BrdU (Figure S4B; Potten et al., 2002). We identified a total of 50 mitotic LRCs, 46 in wild-type tissue and 4 in $Apc^{Min/+}$ (total number of LRC = 2585; wild-type n = 1853; $Apc^{Min/+}$ n = 732). EdU was asymmetrically localized only in dividing LRCs in wild-type tissue. DNA distributions that could be scored unambiguously were almost always in cells in ana- or telophase, whereas metaphase cells constituted the bulk of the cells with ambiguous DNA distributions. In each case where asymmetric DNA localization was unambiguously visible, spindle orientation was perpendicular and the labeled DNA localized to the basal side of the dividing cell (Figure 2). This result established a strong correlation between perpendicularly aligned mitotic spindles and asymmetric retention of labeled DNA. In $Apc^{Min/+}$ tissue, EdU was either distributed symmetrically, consistent with randomly aligned spindles in this tissue, or the localization was ambiguous and could not be clearly classified. Significantly, the dividing cells in wild-type tissue that unambiguously retained EdU label asymmetrically were all located at cell position 4 or below (Figure 2B), suggesting that our labeling experiment targeted both recently identified inter-Paneth cell stem cells and previously identified stem cells at position 4 (Figure S3) and that these cells can selectively retain unreplicated DNA (Barker et al., 2007; Potten et al., 2009).

The correlation between asymmetric distribution of labeled DNA and perpendicular alignment of mitotic spindles, and the decrease in this alignment in $Apc^{Min/+}$ tissue, predicted that LRCs should be more rapidly lost from $Apc^{Min/+}$ tissue. To test this hypothesis, we measured retention and distribution of EdU in 12-week-old $Apc^{Min/+}$ and wild-type littermates after irradiation. The number of basal LRCs per crypt varied between small intestine and colon and between wild-type and $Apc^{Min/+}$

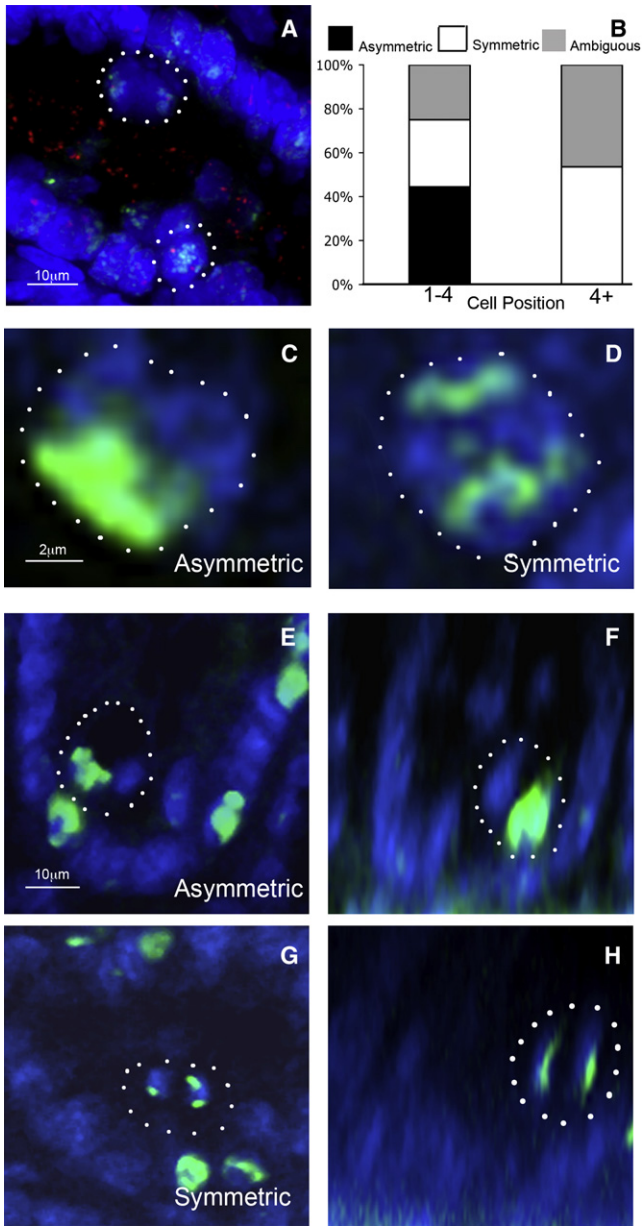

Figure 2. EdU in Dividing, Label-Retaining Cells at the Base of Murine Intestinal Crypts Is Distributed Asymmetrically toward the Basal Surface Only in Wild-Type Tissue

Dividing LRCs in wild-type mouse tissue show asymmetric distribution of EdU.

(A) Symmetric distribution of EdU (green) in mitotic LRCs is visible in 8 μm sections 1 day after EdU injections. Centrosomes were marked with pericentrin antibodies (red) and DAPI was used to stain nuclei (blue). Scale bar represents 10 μm.

(B) With three-dimensional images from whole-mount wild-type tissue, the distribution of EdU in dividing LRCs was scored as asymmetric (black), symmetric (white), or ambiguous (gray) (when a clear assignment could not be made). Asymmetric distribution of EdU was observed in wild-type tissue only in cells at position 4 or below but not above position 4.

(C–H) All but four of the unambiguously identifiable DNA distributions were made in late mitotic cells, whereas cells with DNA distributions that could not be scored clearly tended to be in metaphase. Examples show asymmetric (C, E, F) and symmetric (D, G, H) distribution of EdU (green) in dividing cells in three-dimensional images. Examining images at different angles of rotation helps to unambiguously identify asymmetrically (E, F) and symmetrically (G, H) distributed EdU. Dotted lines mark the circumference of dividing cells. Scale bars represent 2 (C, D) or 10 (E–H) μm.

See also Figures S3 and S4.

intestine. Fewer LRCs were present in $Apc^{Min/+}$ tissue in both regions of the gut (p = 0.002) (Figure 3; Figure S4). Notably, there were no LRCs in adenomatous polyps (Figure 3). Equal uptake of EdU in wild-type and $Apc^{Min/+}$ mice tissue was confirmed by LRC number in mice sacrificed 1 day after completion of injections (Figure S4A).

Cell Shape Is Altered in the Stem Cell Compartment of Precancerous Tissue

The outcome of stem cell divisions is controlled by the coordinated action of (1) extrinsic factors from the surrounding niche that specify stem cell identity and (2) intrinsic cellular factors that act at the centrosome and the cell cortex to orient the plane of cell division with respect to the environment (Pearson and Bloom, 2004). In addition, cell shape may constrain the orientation of mitotic spindles and thus contribute to asymmetric alignment (Théry and Bornens, 2006). To identify potential mechanisms that contribute to the different spindle orientation in wild-type and $Apc^{Min/+}$ tissue, we examined the cellular architecture of the crypt base. We found that cell shape is different in the crypt base in wild-type and $Apc^{Min/+}$ tissue (Figure 4). PAR-3 localization to adherens junctions revealed a regularly spaced, highly crowded arrangement of apical cell junctions between cells in the crypt base in wild-type intestine (Figures 4A–4C). In $Apc^{Min/+}$ tissue, this pattern was irregular, suggesting that the apical surface of cells is highly variable with many much larger apical domains (Figures 4E–4G). This is particularly evident when examining Z-projections (Figures 4B, 4C, 4F, and 4G).

DISCUSSION

The cells that line the intestinal tract are among the most rapidly proliferating cells in the body. The average lifetime of epithelial cells in this tissue is less than 5 days and differentiated cells are continuously replaced from a stable stem cell pool near the base of intestinal crypts. These self-renewing stem cells produce rapidly proliferating transit-amplifying cells that differentiate into the different cell lineages that populate gut epithelium. Just as in skin and the developing nervous system, in gut epithelium this is achieved by divisions of stem cells to produce one daughter stem cell and one differentiating cell (Morrison and Kimble, 2006). However, unlike for skin and the nervous system, asymmetric divisions have not been directly demonstrated in gut epithelium and the importance of such divisions for normal maintenance of this tissue have not been examined. Here, we provide evidence for the preferred perpendicular alignment of mitotic spindles specifically in the stem cell compartment of small and large intestine in mouse and man, by using three-dimensional images of whole-mount tissue. Divisions in the transit-amplifying compartments oriented preferentially symmetrically or showed no bias. Together with our finding that this alignment correlated with the asymmetric segregation of unreplicated DNA strands to

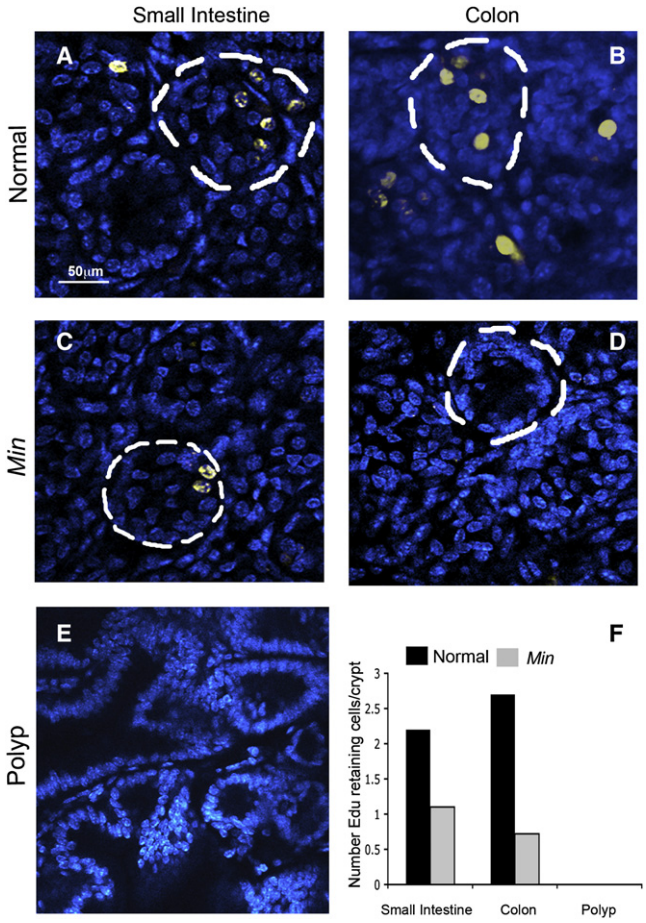

Figure 3. EdU Label-Retaining Cells Are Lost More Rapidly from *Apc*$^{Min/+}$ Precancerous Murine Intestinal Tissue

(A–E) Cross-sections of crypts near the base from small intestine (A, C) and colon (B, D) in wild-type (A, B) and *Apc*$^{Min/+}$ (C, E) tissue show nuclei (blue) and EdU (yellow). (E) No LRCs were detectable in adenomatous polyps of *Apc*$^{Min/+}$ mice. The dotted line in (A)–(D) outlines individual crypts. Scale bar represents 50 μm.

(F) The frequency of LRCs per crypt is reduced in *Apc*$^{Min/+}$ mice and there were no LRCs in adenomatous polyps.

See also Figures S3 and S4.

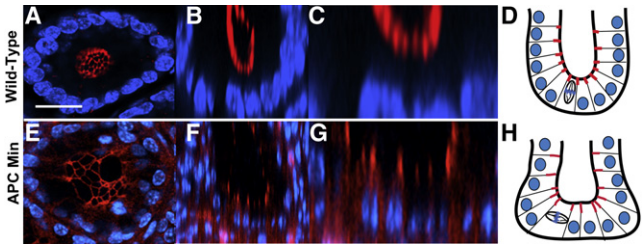

Figure 4. Cell Shape in the Crypt Base Is Altered in *Apc*$^{Min/+}$ Heterozygous Tissue

(A, E) X-Y cross-sections of mouse intestinal crypts stained with PAR-3 antibodies (red) and DAPI (blue) show cell junctions in cells at the crypt base. Wild-type crypts (A) reveal cell junctions positioned at regular intervals indicating uniform size of apically constricted cells. (E) This pattern is much less regular in *Apc*$^{Min/+}$ crypts.

(B, C, F, G) X-Z-sections of the same regions confirm the regular and irregular spacing of cells in wild-type (B, C) and *Apc*$^{Min/+}$ (F, G) crypts. Magnified images (3×) (C, G) make this particularly clear.

Scale bar represents 25 μm (A, B, E, F).

A schematic illustrates how cell shape my affect spindle orientation in the crypt base (D, H). Blue, nuclei; black, cell membrane; red, PAR-3 localization.

the basal side of dividing cells, these data lend support to the idea that Cairns' hypothesis can apply to cells in the stem cell compartment of gut epithelium.

Colorectal cancer (CRC) is the second leading cause of cancer-related death in the western world, making it particularly important to understand the contribution of stem cell biology to the formation of tumors in this tissue. Mutations in *Apc* are common to most colorectal tumors, and evidence for a role of Apc in asymmetric cell division is available from null mutants in yeast and *Drosophila* (Schuyler and Pellman, 2001; Yamashita et al., 2003, 2007). Consistent with a role of asymmetric divisions and the resulting protection of unreplicated DNA in tumorigenesis, adenoma, which usually lack wild-type Apc, do not retain labeled DNA and orient their spindles randomly (Figures 1 and 3). Importantly, we show that heterozygosity of *Apc*, i.e., a precancerous state, already leads to loss of perpendicular alignment of mitotic spindles, which is predicted to mark asymmetric divisions. The conclusion that such perpendicular alignment that places two daughter cells in different environments predicts asymmetric cell fate is formally contingent upon the assumption that the direction of the spindle predicts the distribution of the daughter cells within the interphase crypt column. Only observations in live tissue can resolve whether differently positioned nuclei of daughter cells that result from such asymmetric alignment translate into different fates when their nuclei are repositioned after completing mitosis. However, our finding that loss of perpendicularly oriented divisions correlate with loss of the ability to retain template DNA, specifically in gut epithelial stem cell compartments, suggests that mitotic spindle alignment may predict symmetry of division (Figure 1).

There are a number of potential mechanisms that govern the orientation of mitotic spindles and the outcome of stem cell divisions. These include the coordinated action of (1) extrinsic factors from the surrounding niche that specify stem cell identity and (2) intrinsic cellular factors that act at the centrosome and the cell cortex to orient the plane of cell division with respect to the environment (Pearson and Bloom, 2004). Although in adenomas without any Apc astral microtubules fail to establish adequate cortical attachments, astral microtubules examined in two-dimensional tissue sections of *Apc*$^{Min/+}$ tissue appeared normal, suggesting that cortical connections of mitotic spindles are normal in *Apc* heterozygous tissue (Caldwell et al., 2007; Fleming et al., 2007, 2009). Another mechanism that can contribute to spindle alignment is cell shape, which can constrain the orientation of mitotic spindles and thus contribute to asymmetric alignment (Théry and Bornens, 2006). We found that cell shape in *Apc* heterozygous crypts was more irregular, with less constricted apical domains a common feature. A wider apical domain in the stem cell compartment of *Apc*$^{Min/+}$ tissue might contribute to more random spindle orientation (Figure 4). Mitotic nuclei are positioned toward the apical domain of cells in gut epithelium, and the normally narrow apical space in the

stem cell compartment in wild-type tissue may force perpendicular alignment of mitotic spindles (Figure 4). The wider space in $Apc^{Min/+}$ tissue, on the other hand, could permit parallel orientation more readily (Figure 4). Thus changes in cell shape in $Apc^{Min/+}$ tissue may account for loss of asymmetric orientation in $Apc^{Min/+}$ mice, specifically in the stem cell compartment (Figure 4).

How loss of one allele of *Apc* induces such cell shape changes, whether changes in the signaling activity of β-catenin are to blame, and/or whether other, β-catenin-independent functions like changes in the cytoskeleton are involved will require more detailed experiments. Our results also raise the important question of how selective partitioning of DNA strands is accomplished in this system and how Apc contributes to this process.

Overall, the loss of stem cell protection in cancer-prone tissue has important implications for tumor biology. We propose that this loss increases the probability of generating potentially cancerous cells, which could drive the development of neoplasia. Together with other changes that result from *Apc* heterozygosity, this may tip the balance so that complete loss of Apc and/or other oncogenic mutations can immediately and effectively initiate neoplasia.

EXPERIMENTAL PROCEDURES

Tissue Preparation: Mice

All experiments were performed under the UK Home Office guidelines. Wild-type, $Apc^{Min/+}$ CL57BL/6, and LGR5-GFP mice were sacrificed by cervical dislocation and intestines were removed. 0.5 cm long sections of midjejunum were fixed in methanol at −20°C and stored overnight at −20°C. EdU labeling during postirradiation crypt regeneration was performed on mice irradiated with 8 Gy to the whole body. During regeneration, which takes 2–3 days, EdU at a dose of 1 mg per injection was given at 8 hourly intervals for the first 48 hr postirradiation. The animals were left for 8 days before being sacrificed. During this time, the label present in the majority of the proliferating cells diluted to subthreshold levels, leaving label-retaining cells (LRCs) only in the crypt.

Tissue Preperation: Human

Collection of tissue samples was approved by the Tayside Tissuebank subcommittee of the Local Research Ethics Committee. Normal human samples were obtained from surgical resections for hemicolectomy performed for various indications. After specimen removal, macroscopically normal appearing samples were excised by a consultant pathologist (FAC) and divided into 0.5 cm sections. Human adenoma specimens were also obtained from clinically resected samples. Normal colonic biopsies from familial adenomatous polyposis patients were obtained endoscopically during routine colonoscopy surveillance. All specimens were fixed in −20°C methanol and stored at −20°C overnight.

Immunofluorescence Microscopy

Full details for staining and handling gut tissue samples for multiphoton microscopy have been described previously (Appleton et al., 2009). In brief, methanol-fixed tissue (2 × 2 mm) was rinsed in PBS, then permeabilized. The following primary antibodies were used in combination with appropriate Alexa-Fluor-conjugated secondary antibodies (1:500, Molecular Probes): rabbit polyclonal pericentrin (Abcam ab4448), 1:500; rabbit polyclonal PAR-3 (Upstate 07-330), 1:250. Colonic goblet cells were identified by staining mucous with rhodamine-labeled Dolichos Biflorus Agglutinin lectin at 20 μgmes per ml (RL-1032, Vector Laboratories, Burlingame, USA). Paneth cell lysozyme was stained with a rabbit anti-lysozyme antibody at 1:100 (18-0039, Zymed, Invitrogen, Paisley, UK). Mitotic cells were identified with a rabbit polyclonal antibody against Histone3 - phospho S10 at 1:250 (ab5176, Abcam, Cambridge, UK). DAPI at a concentration of 50 μg/ml was added to the secondary antibody incubation solution. Specimens were rinsed and immersed in increasingly concentrated dilutions of TDE (2,2-thiodiethanol) (10%, 25%, 50%, 97%) in a stepwise manner. Imaging was carried out with a Biorad Radiance 2100MP multiphoton microscope. Stacks were collected at 0.5 μm intervals and were imported into Volocity 4.2 (Improvision) for analysis.

Spindle Orientation Measurements

Spindle orientation was measured with 3-dimensional reconstructions of serial stacks. Spindle angle relative to the crypt center was calculated from the spindle axis vector and a vector from the spindle axis center to the center of the crypt (see Figure 1C). Calculations were performed with Xcode 2.3. Orientations were strictly positive, with a maximum of 90°, which corresponded to spindles parallel to the basal membrane. To confirm accuracy of calculations, measurements were also performed visually by scoring relative spindle orientation by eye in the same images. Scoring by two independent scorers, who were blinded to the origin of the samples, produced the same distribution of spindle orientation angles as the calculations. The position of mitotic cells along the crypt axis was determined by counting cell position from the crypt base.

Statistical Analysis

Results were subjected to statistical analysis with SPSS v16.0 software. Two-tailed p values were calculated with unpaired Student's t tests.

SUPPLEMENTAL INFORMATION

Supplemental Information includes four figures and can be found with this article online at doi:10.1016/j.stem.2009.12.007.

ACKNOWLEDGMENTS

The authors wish to thank all the members of the Light Microscopy Facility of the University of Dundee for their imaging expertise and Professor Mark Chaplain and Ignacio Ramis-Conde (University of Dundee) for developing the Xcode program used to calculate spindle angles. This work was supported by the Cancer Research UK Bobby Moore Fund (A.J.Q.) and a programme grant from Cancer Research UK (I.S.N.).

Received: June 30, 2009
Revised: October 26, 2009
Accepted: December 15, 2009
Published: February 4, 2010

REFERENCES

Ahringer, J. (2003). Control of cell polarity and mitotic spindle positioning in animal cells. Curr. Opin. Cell Biol. *15*, 73–81.

Appleton, P.L., Quyn, A.J., Swift, S., and Näthke, I. (2009). Preparation of wholemount mouse intestine for high-resolution three-dimensional imaging using two-photon microscopy. J. Microsc. *234*, 196–204.

Barker, N., van Es, J.H., Kuipers, J., Kujala, P., van den Born, M., Cozijnsen, M., Haegebarth, A., Korving, J., Begthel, H., Peters, P.J., and Clevers, H. (2007). Identification of stem cells in small intestine and colon by marker gene Lgr5. Nature *449*, 1003–1007.

Barker, N., Ridgway, R.A., van Es, J.H., van de Wetering, M., Begthel, H., van den Born, M., Danenberg, E., Clarke, A.R., Sansom, O.J., and Clevers, H. (2009). Crypt stem cells as the cells-of-origin of intestinal cancer. Nature *457*, 608–611.

Bjerknes, M., and Cheng, H. (1989). Mitotic orientation in three dimensions determined from multiple projections. Biophys. J. *55*, 1011–1015.

Cairns, J. (1975). Mutation selection and the natural history of cancer. Nature *255*, 197–200.

Caldwell, C.M., Green, R.A., and Kaplan, K.B. (2007). APC mutations lead to cytokinetic failures in vitro and tetraploid genotypes in Min mice. J. Cell Biol. *178*, 1109–1120.

Fleming, E.S., Zajac, M., Moschenross, D.M., Montrose, D.C., Rosenberg, D.W., Cowan, A.E., and Tirnauer, J.S. (2007). Planar spindle orientation and asymmetric cytokinesis in the mouse small intestine. J. Histochem. Cytochem. *55*, 1173–1180.

Fleming, E.S., Temchin, M., Wu, Q., Maggio-Price, L., and Tirnauer, J.S. (2009). Spindle misorientation in tumors from APC(min/+) mice. Mol. Carcinog. *48*, 592–598.

Green, R.A., Wollman, R., and Kaplan, K.B. (2005). APC and EB1 function together in mitosis to regulate spindle dynamics and chromosome alignment. Mol. Biol. Cell *16*, 4609–4622.

Hans, F., and Dimitrov, S. (2001). Histone H3 phosphorylation and cell division. Oncogene *20*, 3021–3027.

Judson, H., Stewart, A., Leslie, A., Pratt, N.R., Baty, D.U., Steele, R.J., and Carey, F.A. (2006). Relationship between point gene mutation, chromosomal abnormality, and tumour suppressor gene methylation status in colorectal adenomas. J. Pathol. *210*, 344–350.

Li, Z., and Näthke, I.S. (2005). Tumor-associated NH2-terminal fragments are the most stable part of the adenomatous polyposis coli protein and can be regulated by interactions with COOH-terminal domains. Cancer Res. *65*, 5195–5204.

Li, Z., Kroboth, K., Newton, I.P., and Näthke, I.S. (2008). Novel self-association of the APC molecule affects APC clusters and cell migration. J. Cell Sci. *121*, 1916–1925.

Morrison, S.J., and Kimble, J. (2006). Asymmetric and symmetric stem-cell divisions in development and cancer. Nature *441*, 1068–1074.

Pearson, C.G., and Bloom, K. (2004). Dynamic microtubules lead the way for spindle positioning. Nat. Rev. Mol. Cell Biol. *5*, 481–492.

Potten, C.S., Owen, G., and Booth, D. (2002). Intestinal stem cells protect their genome by selective segregation of template DNA strands. J. Cell Sci. *115*, 2381–2388.

Potten, C.S., Gandara, R., Mahida, Y.R., Loeffler, M., and Wright, N.A. (2009). The stem cells of small intestinal crypts: Where are they? Cell Prolif. *42*, 731–750.

Schuyler, S.C., and Pellman, D. (2001). Search, capture and signal: Games microtubules and centrosomes play. J. Cell Sci. *114*, 247–255.

Théry, M., and Bornens, M. (2006). Cell shape and cell division. Curr. Opin. Cell Biol. *18*, 648–657.

Yamashita, Y.M., Jones, D.L., and Fuller, M.T. (2003). Orientation of asymmetric stem cell division by the APC tumor suppressor and centrosome. Science *301*, 1547–1550.

Yamashita, Y.M., Mahowald, A.P., Perlin, J.R., and Fuller, M.T. (2007). Asymmetric inheritance of mother versus daughter centrosome in stem cell division. Science *315*, 518–521.